A Unified Energy-Based Control Strategy for Modular Multilevel Converters in Multi-Terminal DC Grids Under Diverse Network Configurations

Shabab Samimi · **Saeed Hosseinnataj** · **Reza Farajpour** · **Johan Boukhenfouf** · **François Gruson** · **Xavier Guillaud** · **Frédéric Colas**

Abstract This paper investigates energy-based station-level control of modular multilevel converters (MMCs) in multi-terminal high-voltage direct-current (MTDC) grids with heterogeneous DC-side configurations. Reliable station-level control is required to ensure stable power flow under varying operating modes and AC- and DC-side disturbances. In practical MTDC systems, MMC stations must accommodate DC-voltage and power control while interfacing with diverse DC infrastructures, including cables, overhead lines, and DC circuit breakers (DCCBs). However, most existing control approaches rely on a single averaged-arm MMC model and assume fixed DC-side dynamics, limiting their applicability during transients and across different network characteristics. To address these challenges, a unified station-level modeling and control framework is proposed to explicitly accounts MMC operating modes and key DC-side elements by enabling effective decoupling between internal MMC dynamics and DC-side behavior. Time-domain simulations of a representative MMC station validate the effectiveness of the proposed approach.

1 Introduction

The rapid integration of large-scale renewable energy sources, together with the growing need for efficient long-distance transmission and asynchronous interconnection of power systems, has positioned voltage-source-converter-based high-voltage direct-current (VSC-HVDC) technology at the core of future power grids [1]. The continued expansion of HVDC links has led to the emergence of MTDC grids, which enable meshed interconnections of asynchronous AC systems while providing enhanced controllability, reliability, and utilization of transmission corridors [2]. Despite this advantages, many technical challenges in MTDC systems originate at the converter station level and remain equally relevant in point-to-point HVDC schemes. In this context, converter topology and station-level control play a decisive role in overall system dynamic performance under both normal and disturbed conditions. Among VSC technologies, the MMC has become the preferred solution for HVDC applications due to its superior power quality, modular scalability, flexible power-flow control, and low harmonic distortion [3]. A key challenge in HVDC operation is maintaining stable and coordinated performance under heterogeneous DC infrastructures and varying operating conditions. Long cable-based DC networks exhibit capacitive-dominant behavior, whereas short cables and overhead lines are inductive-dominant and more susceptible to transient faults and stringent protection requirements. To ensure safe and reliable operation, MTDC grids increasingly rely on fast DCCBs equipped with series reactors to limit fault currents [4].While essential for protection, these inductive elements significantly alter DC-side dynamics and must be explicitly considered in station-level control design. As demonstrated in [5] the DCCB inductance introduces low-frequency poles that may cause voltage-oscillations and even DC-voltage stability throughout the MTDC network. Therefore, MMC station-level controllers must remain effective across both capacitive-dominant DC networks and inductive-dominant networks. Although extensive research has addressed modeling and control of MMC-based MTDC systems [6], most existing station-level control strategies are derived for specific operating modes and DC-network

S.Samimi
ESME, ESME Research Lab, F-59800 Lille, France.
e-mail: shabab.samimi@esme.fr

S. Hosseinnataj · R.Farajpour · J.Boukhenfouf · F. Gruson · X. Guillaud · F. Colas
Univ. Lille, Arts et Métiers Institute of Technology, Centrale Lille, Junia, ULR 2697 - L2EP, F-59000 Lille, France
e-mail: francois.gruson@ensam.eu

conditions, often neglecting the wide range of DC-side dynamic behaviors encountered in practical MTDC grids.As a result, interactions between station-level control and DC-side dynamics particularly in networks combining DC cables, overhead lines, and DCCBs remain insufficiently addressed. This paper focuses on the MMC station responsible for DC-voltage regulation, which plays a central role in DC-network stability and power-flow coordination.

To address this gap, a unified MMC station-level modeling and control framework is proposed that explicitly decouples internal MMC dynamics from DC-side behavior, ensuring consistent control performance across heterogeneous DC-network configurations.The principal contributions of this work are :

1. A comprehensive averaged-arm modeling framework for an MMC operating in DC-voltage regulation mode is developed, which explicitly captures diverse DC-side configurations, including capacitive-dominant DC networks (e.g., long DC cables) and inductive-dominant networks (e.g., short DC cables or overhead DC lines). The proposed model also explicitly incorporates the series inductance L_{dc} and resistance R_{dc} of the DCCBs.
2. Based on this model, a unified MMC station level control strategy is designed that ensures consistent DC-voltage and DC-current dynamic performance across different DC-side configurations, while effectively decoupling the internal MMC dynamics from the DC-network behavior.

The remainder of this paper is organized as follows. Section II presents the averaged-arm MMC model and associated inner current control loops. Section III introduces the proposed unified station-level control strategy. Section IV evaluates controller performance through time-domain simulations under different DC-side configurations. Section V concludes the paper.

2 MMC modeling and inner current loops

In this section, a unified averaged-arm MMC model is developed for a converter station operating in DC-voltage regulation mode under different DC side configurations. In HVDC links or in MTDC grids, at least one converter is typically assigned to establish the DC-voltage reference, while the remaining stations regulate their power exchange with the connected AC networks. Accordingly, the MMC model and the associated inner current control loops are formulated to reflect the operational role of the DC-voltage–controlling station. To assess the influence of DC network dynamics on station-level control, two representative DC-side configurations are considered, as illustrated in Fig. 1.

In DC-voltage control mode, the MMC regulates the DC-link voltage to the reference value V_{DC}^{*}, while the DC current is imposed by other MMC stations operating in power-control

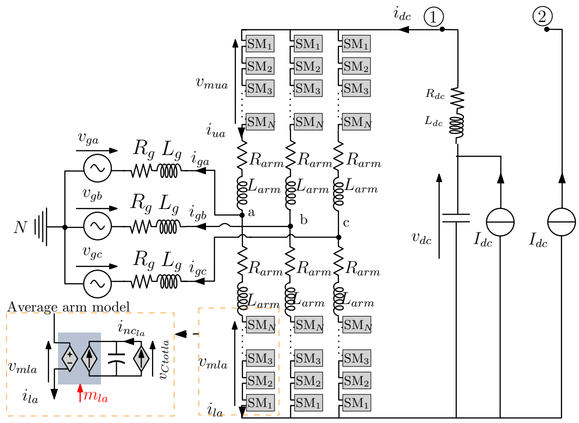

Fig. 1 MMC model under different DC network configurations

mode. In such stations,the DC current reference is derived from the active-power set-point according to $i_{DC}^{\star} = \frac{P_{AC}^{\star}}{V_{DC}^{\star}}$. Consequently, from the perspective of the DC-voltage–regulating MMC, the remaining power-controlled stations are represented as a DC current source. The first DC-side configuration corresponds to a capacitive-dominant network, representative of cable-based DC systems in which the distributed capacitance of the DC cables cannot be neglected and is modeled by an equivalent DC-link capacitance associated with the voltage V_{dc} . When DCCBs are installed,the series impedance introduced by the DCCB, characterized by L_{dc} and R_{dc} must be taken into account.

The second configuration represents an inductive-dominant DC network, typical of short DC cables or overhead DC transmission lines, with or without DCCBs. In this case, the DC current is dictated by other MMC stations operating in power-control mode and the DC network exhibits inductive dominated behavior which can be represented as a controlled current source I_{DC}.

2.1 MMC average arm model

By explicitly considering both cases, the proposed framework establishes a unified representation of the MMC–DC network interface, providing a consistent foundation for station-level modeling and control irrespective of the surrounding DC network characteristics. On this basis, a well-known MMC average arm model is considered, in which each arm submodule stack is replaced by an equivalent arm model consisting of an averaged switching function and an equivalent capacitance [7], as shown in Fig. 1. This model assumes that capacitor voltages are well balanced by the control operation (i.e. $v_{cSM1} = v_{cSM2} = \cdots = v_{cSMN} = \frac{v_{ctot}}{N}$), and this assumption allows considering an equivalent capacitor ($C_{tot} = C_{SM}/N$). Where N is the number of submodules that can reach hundreds in number in HVDC applications. Based on modeling method above, 6 modulation indexes (m_{ui},m_{li}) as duty cycle for equivalent chopper are defined. Next, based on average arm model, the equations below can be expressed for each equivalent arm of the MMC:

$$\begin{aligned} v_{mu/li} &= m_{u/li} v_{ctotu/li} \quad i \in \{a,b,c\} \\ i_{cu/li} &= m_{u/li} i_{ctotu/li} = C_{eq-i} \frac{dv_{ctotu/li}}{dt} \end{aligned} \tag{1}$$

A classical state-variable transformation is then employed to decouple the AC and DC variables:

$$\begin{aligned} i_{diff_i} &= \frac{i_{ui}+i_{li}}{2} \\ v_{diff_i} &= \frac{v_{mui}+v_{mli}}{2} \quad |v_{v_i} = \frac{v_{mli}-v_{mui}}{2} \end{aligned} \tag{2}$$

2.2 Inner current loop

For the configuration 1, the application of (2) enables a structured separation between the AC-side and DC-side dynamics of the MMC. As a result the system can be represented by the following set of decoupled dynamic equations. The per-phase differential current dynamics on the DC side are given by:

$$\frac{v_{dc}}{2} - v_{diff_i} = L_{arm} \frac{di_{diffi}}{dt} + R_{arm} i_{diffi} + L_{dc} \frac{di_{dc}}{dt} + R_{dc} i_{dc} \tag{3}$$

while the per-phase AC-side grid current dynamics are expressed as:

$$v_{vi} - v_{gi} = R_{eq} i_{gi} + L_{eq} \frac{di_{gi}}{dt} \tag{4}$$

Where $L_{eq} = L_g + \frac{L_{arm}}{2}$ and $R_{eq} = R_g + \frac{R_{arm}}{2}$

Expressing the per-phase AC current dynamics in the dq frame leads to (5), which serve as the basis for the design of the AC inner current controller.

$$\begin{cases} v_{vd} - v_{gd} = R_{eq} i_{gd} + L_{eq} \dfrac{di_{gd}}{dt} + \omega L_{eq} i_{gq} \\ v_{vq} - v_{gq} = R_{eq} i_{gq} + L_{eq} \dfrac{di_{gq}}{dt} + \omega L_{eq} i_{gd} \end{cases} \tag{5}$$

It is important to note that the AC-side dynamics in (5) are independent of the DC-side configuration, including the presence of DCCB-associated series impedance. Consequently, the AC grid current dynamics remain unchanged when DC circuit breakers are considered. Using an inversion-based control approach, the corresponding inner-level control structure can be systematically derived. More details can be find in [7]. On the DC side, the per-phase differential current dynamics in (3) reveal a direct coupling between the DC current and the per-phase differential currents, as imposed by Kirchhoff's current law. To enable independent regulation of the inner MMC currents from the DC current dynamics, an additional change of variables is introduced in which the phase differential currents are expressed in terms of circulating current components obtained from phase current differences (e.g., a–c and b–c), together with a common-mode component defined by their sum (a+b+c). Here i^x_{cir} and i^y_{cir} represent internal circulating currents within the converter. This transformation as noted by matrix M_1 in (6), isolates the internal MMC current dynamics from the DC current dynamics.

$$\begin{cases} \begin{bmatrix} i^x_{cir} \\ i^y_{cir} \end{bmatrix} = \mathbf{M}_1 \begin{bmatrix} i_{diffa} \\ i_{diffb} \\ i_{diffc} \end{bmatrix} \qquad Where \quad \mathbf{M}_1 = \begin{bmatrix} 1 & 0 & -1 \\ 0 & 1 & -1 \end{bmatrix} \\ i_{dc} = i_{diffa} + i_{diffb} + i_{diffc} \end{cases} \tag{6}$$

These internal circulating currents, flow between converter legs (a-c or b-c) and they are independent of the nature of the DC side. Accordingly, the voltages v^x_{cir} and v^y_{cir} that drive these currents are also referred to as circulating voltages.

$$\begin{cases} \begin{bmatrix} v^x_{cir} \\ v^x_{cir} \end{bmatrix} = \mathbf{M}_1 \begin{bmatrix} v_{diffa} \\ v_{diffb} \\ v_{diffc} \end{bmatrix} \\ v_{mdc} = \dfrac{1}{3}(v_{diffa} + v_{diffb} + v_{diffc}) \end{cases} \tag{7}$$

Based on equation (6) and (7) MMC DC side loop leads to:

$$\begin{cases} v^x_{\text{cir}} &= -L_{\text{arm}} \dfrac{di^x_{\text{cir}}}{dt} - R_{\text{arm}} i^x_{\text{cir}} \\ v^y_{\text{cir}} &= -L_{\text{arm}} \dfrac{di^y_{\text{cir}}}{dt} - R_{\text{arm}} i^y_{\text{cir}} \\ \dfrac{v_{\text{dc}}}{2} - v_{m_{dc}} &= \left(L_{\text{dc}} + \dfrac{L_{\text{arm}}}{3}\right) \dfrac{di_{\text{dc}}}{dt} + \left(R_{\text{dc}} + \dfrac{R_{\text{arm}}}{3}\right) i_{\text{dc}} \end{cases} \tag{8}$$

As discussed previously, the internal circulating currents i^x_{cir} and i^y_{cir} which circulate between legs a-c and b-c respectively, are inherently independent of the nature of the DC-side nature. Consequently, their dynamics can be derived using the same formulation as in (8), and the associated circulating-current control structure can be directly reused without modification. Owing to the current-dominated nature of the DC network in Configuration 2, explicit DC-current regulation at the MMC station level is not possible, as the DC current (I_{dc}) is dictated by the external DC-side conditions which leads to $v_{mdc_0} = \frac{1}{3}(v_{dc_0})$.

By applying the model inversion, a unified control law can be derived. In this framework, the references for the AC and DC side currents are generated by the energy control loop, which is described in detail in the following section.

3 Unified Energy-Based control

Based on the unified MMC model introduced in Section II, this section presents the proposed energy-based control strategy. The insertion of stacked submodules leads to an indirect energy conversion process in which the instantaneous AC and DC powers are generally unequal, resulting in internal energy deviations that must be regulated to avoid arm-voltage depletion and ensure stable operation. To this end, the high-level controller generates AC and DC current references that satisfy external active-power requirements while maintaining internal energy balance. The resulting control architecture follows a cascaded structure, where power and energy regulation constitute the outer loops, and AC-grid current and differential-current control are implemented in the inner loops. The conventional energy based control, as investigated in [8], is widely adopted in HVDC grid applications. In this approach, all capacitor related energy variables of the MMC are controlled. Since considering the differential currents contain both DC and AC components, the total (Horizontal) and differential (Vertical) energy stored in each leg of the MMC can be defined as (9) and (10) respectively:

$$\begin{aligned} < \frac{dW_i^{\Sigma}}{dt} >_T &=< \frac{1}{2}C_{\text{tot}}\frac{d}{dt}(V^2_{\text{ctot-ui}} + V^2_{\text{ctot-li}}) >_T \\ &=< v_{dc} i_{diffi-dc} >_T - < p_{aci} >_T \end{aligned} \tag{9}$$

$$\begin{aligned} < \frac{dW_i^{\Delta}}{dt} >_T &=< \frac{1}{2}C_{\text{tot}}\frac{d}{dt}(V^2_{\text{ctot-ui}} - V^2_{\text{ctot-li}}) >_T \\ &= -2 < i_{diffi_{ac}} v_{gi} >_T \end{aligned} \tag{10}$$

In the MMC arm average model, six state variables associated with the submodule capacitor voltages must be regulated, requiring six independent control inputs to ensure full controllability of the converter energy. To address this requirement, a decoupled representation of the differential current is adopted. The differential current is decomposed into DC and AC components, while the AC component is further expressed in terms of positive- and negative-sequence components. This formulation introduces additional control degrees of freedom while preventing AC zero-sequence current injection into the DC side, as proposed in [9]. The relationship between these components and the regulation of the different energy terms will be detailed in the following section. The differential currents are then expressed as follows:

$$\begin{aligned} i_{\text{diff},i} &= i^{\text{dc}}_{\text{diff},i} + i^{\text{ac}+}_{\text{diff}}\sqrt{2}\cos\big(\theta_g + \Phi_x^{+}\big) \\ &\quad + i^{\text{ac}-}_{\text{diff}}\sqrt{2}\cos\big(\theta_g + \Phi_x^{-}\big). \end{aligned} \tag{11}$$

In order to decouple DC current and MMC circulating current similar to the differential current considerations the circulating currents i^x_{cir} , i^y_{cir} can be decomposed into DC and AC components, which provides five independent control variables. However, the DC-link current i_{dc} can only contain a DC component, resulting in a missing control degree of freedom. To address this issue, positive and negative sequence components are introduced into the AC circulating-currents. This leads to the following definitions of the circulating currents:

$$\begin{cases} i^x_{\text{cir}} = i^x_{\text{cir-dc}} + I^x_{\text{cir-ac}\oplus}\sqrt{2}\cos\big(\theta_g + \Phi^x_{\oplus}\big) + I^x_{\text{cir-ac}\ominus}\sqrt{2}\cos\big(\theta_g + \Phi^x_{\ominus}\big) \\ i^y_{\text{cir}} = i^y_{\text{cir-dc}} + I^y_{\text{cir-ac}\oplus}\sqrt{2}\cos\big(\theta_g + \Phi^y_{\oplus}\big) + I^y_{\text{cir-ac}\ominus}\sqrt{2}\cos\big(\theta_g + \Phi^y_{\ominus}\big) \end{cases} \tag{12}$$

This approach enables a clear decoupling between the DC-link current and the MMC circulating currents and restores full controllability of the converter energy as detailed in the next subsections.The overal control structure for DC-voltage regulating MMC station is provided in Fig.2.

a) Horizontal energy balancing

In the proposed control strategy, the energy balance of the MMC leg capacitors is enforced by using the same transformation matrix that is applied to the differential currents (6). Accordingly, the stored leg powers equation (9) is transformed as:

$$\begin{cases} \begin{bmatrix} < \frac{dW_x^{\Sigma}}{dt} >_T \\ < \frac{dW_y^{\Sigma}}{dt} >_T \end{bmatrix} = \begin{bmatrix} < v_{dc} i^x_{cir_{dc}} >_T - < p^x_{ac} >_T \\ < v_{dc} i^y_{cir_{dc}} >_T - < p^y_{ac} >_T \end{bmatrix} \\ < \dfrac{dW^{\Sigma}_{tot}}{dt} >_T =< v_{dc} i_{dc} >_T - < p_{ac} >_T \end{cases} \tag{13}$$

Here W^{Σ}_{tot} denotes the total energy stored in the MMC capacitors,whereas W_x^{Σ} and W_y^{Σ} represent the stored energy differences between leg pairs a-c and b-c, respectively. Unlike convention energy-based control approaches, the proposed model decoupled these three energy states: The difference leg energy states, W_x^{Σ} and W_y^{Σ} can be regulated independently by commanding the circulation DC current components $i^x_{cir_{dc}}$ and $i^y_{cir_{dc}}$, respectively. In addition, the total stored energy (W^{Σ}_{tot}) may be regulated either through the DC power or through the AC power. However, when the MMC operates as a DC-voltage regulating station, regultion of W^{Σ}_{tot} is restricted to the AC side.

Consequently, the capability to control the total MMC energy through the AC power while keeping the phase-energy balances W_x^{Σ} and W_y^{Σ} independent of the DC-link voltage is crucial for reliable operation of MMCs linked by HVDC cables. This decoupling ensures that each converter can maintain its internal energy balance irrespective of fluctuations in the DC-link voltage, while simultaneously ensuring the required power exchange with the AC network.

b) Vertical energy balancing

In contrast to the W^{Σ}_{tot} model, the energy balancing between the MMC arm capacitors W_i^{Δ} cannot be directly performed through the same transformation due to the circulating currents coupling. Accordingly to (11) the DC component of

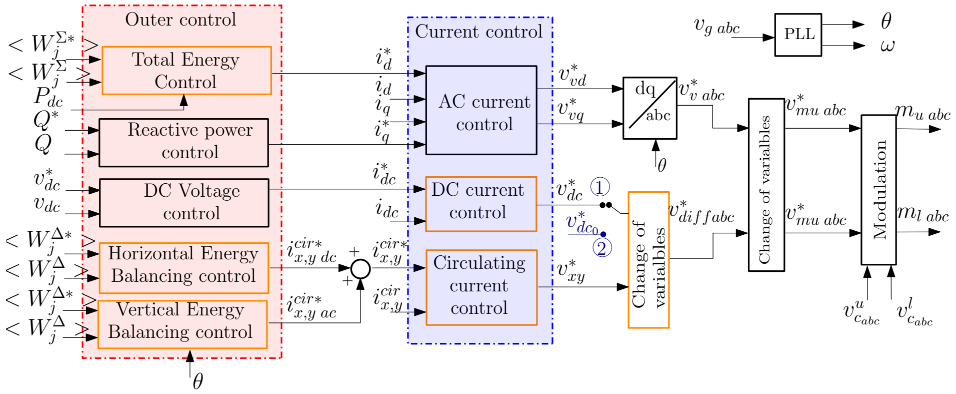

Fig. 2 Unified MMC Control Structure for DC-voltage regulating station

differential currents have no effect on the dynamics of arm-energy states W_i^Δ and the direct and inverse sequences without zero-sequence components in the AC components of differential currents should be applied. Then the equations (10) and (11) lead to:

$$\begin{cases} < \dfrac{dW_a^\Delta}{dt} >_T = -2V_g(i_{\text{diffi-ac}\oplus}\cos\Phi_\oplus + i_{\text{diffi-ac}\ominus}\cos\Phi_\ominus) \\ < \dfrac{dW_b^\Delta}{dt} >_T = -2V_g\left(i_{\text{diffi-ac}\oplus}\cos\Phi_\oplus + i_{\text{diffi-ac}\ominus}\cos(\Phi_\ominus + \dfrac{4\pi}{3})\right) \\ < \dfrac{dW_c^\Delta}{dt} >_T = -2V_g\left(i_{\text{diffi-ac}\oplus}\cos\Phi_\oplus + i_{\text{diffi-ac}\ominus}\cos(\Phi_\ominus - \dfrac{4\pi}{3})\right) \end{cases} \tag{14}$$

Subsequently, the Clarke transformation (M_2) is applied to express the currents in the d–q frame for both positive and negative sequence components, resulting in a decoupled representation of the dynamics associated with each arm-energy state W_i^Δ:

$$\begin{cases} < \dfrac{dW_\gamma^\Delta}{dt} >_T = -2V_g I_{\text{diffd}\ominus}, \\ < \dfrac{dW_\Psi^\Delta}{dt} >_T = -2V_g I_{\text{diffq}\ominus}, \\ < \dfrac{dW_{tot}^\Delta}{dt} >_T = -2V_g I_{\text{diffd}\oplus}. \end{cases} \quad \mathbf{M}_2 = \begin{bmatrix} 2 & -1 & -1 \\ 0 & -\frac{1}{\sqrt{3}} & \frac{1}{\sqrt{3}} \\ \frac{1}{3} & \frac{1}{3} & \frac{1}{3} \end{bmatrix} \tag{15}$$

The model derived in the preceding section reveals that the positive sequence quadrature component of the differential current emerges as a control degree of freedom. By inverting the generalized energy based model equations (9)-(15) the associated generalized energy based control architecture is obtained as shown in Fig. 3. In the proposed control scheme, all energy signals are filtered with Moving-Average Filters (MAF) [10] to suppress measurement noise and to provide smooth reference generation. Because the AC and DC powers are assumed constant over the control horizon, the total stored energy can be obtained directly as the sum of the energies stored in the equivalent arm capacitors.

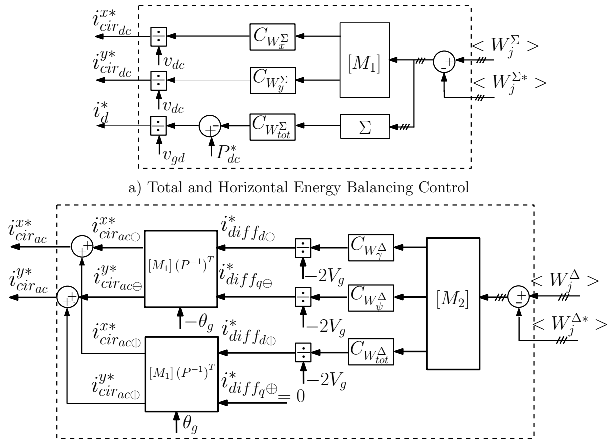

a) Total and Horizontal Energy Balancing Control

b) Vertical Energy Balancing Control

Fig. 3 Block diagram of energy control loop in the unified control strategy

4 Case study and Simulation results

To evaluate the proposed control strategy, time-domain simulations were performed in MATLAB/Simulink for an MMC connected to the DC-side configurations introduced in Section II. The system consists of a single MMC operating in DC-voltage regulation mode and interfaced with a stiff AC grid and a DC link. The main parameters are summarized in Table 1.

Fig. 4 shows the dynamic responses under three representative scenarios. Cases (1-a) and (1-b) correspond to a capacitive dominant DC network without and with the DCCB series inductance L_{dc}, while case (2) represents an inductive dominant DC network. A 0.2 pu step is applied to the DC current reference at $t = 0.1s$, followed by a change in the arm capacitor voltages $V^*_{cu/l}$ references at $t = 0.45s$ to assess the internal energy regulation capability of the proposed controller. The results show that in all cases the DC current accurately tracks its reference, while the AC active power, the d-axis AC current component, and the arm capacitor voltages remain well regulated. The comparison between cases (1-a) and (1-b)

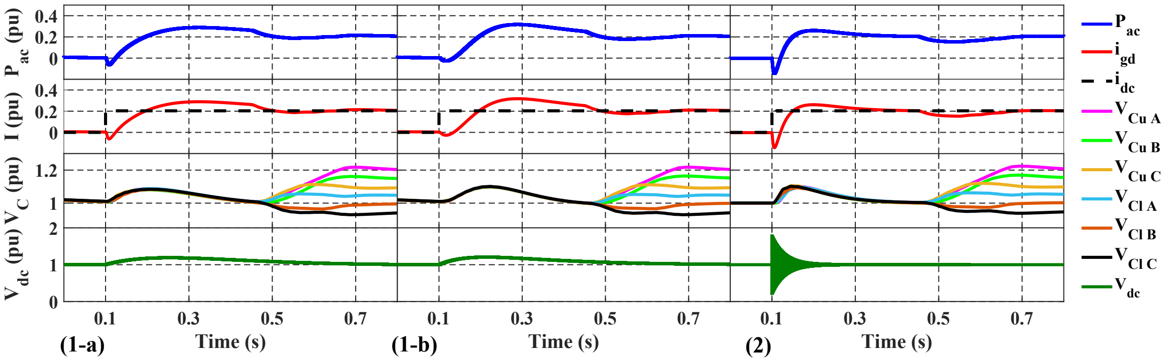

Fig. 4 Simulation results of the unified control strategy for an MMC connected to the two DC-side configurations

Table 1 Case study Parameters

Parameter	Value (SI)
Nominal frequency	50 Hz
Nominal power	1×10^9 W
Grid nominal phase-to-phase voltage	400×10^3 V
AC grid resistance (R_g)	5 mΩ
AC grid inductance (L_g)	50 mH
Nominal DC voltage (V_{dc})	640×10^3 V
Arm resistance (R_{arm})	512 mΩ
Arm inductance (L_{arm})	58.7 mH
DC line inductance (L_{dc})	200 mH
Capacitive energy constant of DC cable (H_c)	20 ms
Converter energy constant (H_c)	40 ms
Inner currents controllers time response	5 ms
Energy controllers time response	150 ms
DC-voltage controller time response	50 ms

shows that inclusion of L_{dc} does not introduce oscillatory behavior. Moreover, in case (2), DC-side voltage oscillations do not affect the AC current or to the internal capacitor voltages. These results confirm stable energy regulation and effective decoupling between the DC-link dynamics and the internal circulating currents under different DC-network conditions.

5 Conclusions

This paper presented a unified station-level energy-based control framework for MMCs operating in MTDC grids with heterogeneous DC-network characteristics. A unified averaged-arm MMC model was developed to capture both capacitive and inductive dominant DC-network dynamics, including the effects of DC circuit breakers. Based on this model, a unified energy-based control architecture was formulated to decouple MMC internal dynamics from DC-side behavior while ensuring robust regulation of internal energy and AC/DC currents. Time-domain simulation results demonstrate that the proposed approach overcomes key limitations of conventional station-level controllers, which are typically tailored to specific operating modes or DC-network conditions. Overall, the proposed framework provides a systematic and scalable solution for MMC-based MTDC systems and supports the reliable and coordinated operation of future meshed HVDC grids.

Acknowledgments This project has received funding from the European Union's Horizon Europe research and innovation programme under grant agreement No 101160687 (PROSECCO).

References

1. D. Van Hertem, O. Gomis-Bellmunt, and J. Liang, *HVDC Grids: For Offshore and Supergrid of the Future*. Hoboken, NJ, USA: Wiley-IEEE Press, 2016.
2. W. Feng, L. A. Tuan, L. B. Tjernberg, A. Mannikoff, and A. Bergman, "A new approach for benefit evaluation of multiterminal VSC-HVDC using a proposed mixed AC/DC optimal power flow," *IEEE Transactions on Power Delivery*, vol. 29, no. 1, pp. 432–443, 2014.
3. J. A. Ansari, C. Liu, and S. A. Khan, "MMC-based MTDC grids: A detailed review on issues and challenges for operation, control, and protection schemes," *IEEE Access*, vol. 8, pp. 168 154–168 165, 2020.
4. F. Mohammadi, K. Rouzbehi, M. Hajian, K. Niayesh, G. B. Gharehpetian, H. Saad, M. Hasan Ali, and V. K. Sood, "Hvdc circuit breakers: A comprehensive review," *IEEE Transactions on Power Electronics*, vol. 36, no. 12, pp. 13 726–13 739, 2021.
5. W. Wang, M. Barnes, O. Marjanovic, and O. Cwikowski, "Impact of dc breaker systems on multiterminal vsc-hvdc stability," *IEEE Transactions on Power Delivery*, vol. 31, no. 2, pp. 769–779, 2016.
6. P. Rodriguez and K. Rouzbehi, "Multi-terminal dc grids: challenges and prospects," *Journal of Modern Power Systems and Clean Energy*, vol. 5, no. 4, pp. 515–523, 2017.
7. S. Samimi, F. Gruson, P. Delarue, and X. Guillaud, "Synthesis of different types of energy based controllers for a modular multilevel converter integrated in an hvdc link," in *11th IET International Conference on AC and DC Power Transmission*, 2015, pp. 1–7.
8. E. Sánchez-Sánchez, E. Prieto-Araujo, A. Junyent-Ferré, and O. Gomis-Bellmunt, "Analysis of mmc energy-based control structures for vsc-hvdc links," *IEEE Journal of Emerging and Selected Topics in Power Electronics*, vol. 6, no. 3, pp. 1065–1076, 2018.
9. K. Shinoda, J. Pou, G. Konstantinou, and V. G. Agelidis, "Energy difference controllers for modular multilevel converters without dc current perturbations," *IEEE Transactions on Power Electronics*, vol. 31, no. 2, pp. 1182–1194, 2016.
10. S. Golestan, M. Ramezani, J. M. Guerrero, F. D. Freijedo, and M. Monfared, "Moving average filter based phase-locked loops: Performance analysis and design guidelines," *IEEE Transactions on Power Electronics*, vol. 29, no. 6, pp. 2750–2763, 2014.